



FULL LENGTH ARTICLE

# Monogenic deficiency in murine intestinal Cdc42 leads to mucosal inflammation that induces crypt dysplasia



Dongsheng Zhang <sup>a,b,c,1</sup>, Wenjuan Tang <sup>c,d,1</sup>, Haitao Niu <sup>e,f</sup>,  
William Tse <sup>a,b</sup>, Hai-Bin Ruan <sup>g</sup>, Helmut Dolznig <sup>h</sup>,  
Thomas Knösel <sup>i</sup>, Friedrich Karl-Heinz <sup>j</sup>, Madeleine Themanns <sup>k</sup>,  
Jiang Wang <sup>m</sup>, Mingquan Song <sup>n</sup>, Lee Denson <sup>c</sup>, Lukas Kenner <sup>o</sup>,  
Richard Moriggl <sup>p,q,r</sup>, Yi Zheng <sup>s</sup>, Xiaonan Han <sup>a,b,\*</sup>

<sup>a</sup> Division of Hematology and Oncology, Division of Cancer Biology, Department of Medicine, MetroHealth Medical Center (MHMC), Case Western Reserve University (CWRU), School of Medicine, Cleveland, OH 44109, USA

<sup>b</sup> Cancer Genomics and Epigenomics Program, Case Comprehensive Cancer Center, Case Western Reserve University (CWRU), Cleveland, OH 44106, USA

<sup>c</sup> Division of Gastroenterology, Hepatology and Nutrition, Cincinnati Children's Hospital Medical Center (CCHMC), Cincinnati, OH 45229, USA

<sup>d</sup> Children's Hospital of Fudan University, Shanghai 201102, China

<sup>e</sup> School of Medicine, Jinan University, Guangzhou, Guangdong 510632, China

<sup>f</sup> Laboratory Animal Science (ILAS), Chinese Academy of Medical Science (CAMS) and Peking Union Medical College (PUMC), Beijing 100006, China

<sup>g</sup> Department of Integrative Biology and Physiology, University of Minnesota Medical School, Minneapolis, MI 55455, USA

<sup>h</sup> Institute of Medical Genetics, Medical University of Vienna, Vienna 1040, Austria

<sup>i</sup> Institute of Pathology, Ludwig-Maximilians-University Munich, Munich 80539, Germany

<sup>j</sup> Institute of Biochemistry II, University Hospital Jena, Jena 07743, Germany

<sup>k</sup> Laboratory Animal Pathology, University of Veterinary Medicine Vienna, Vienna 1210, Austria

<sup>m</sup> Department of Pathology, University of Cincinnati, Cincinnati, OH 45221, USA

<sup>n</sup> Department of Gastroenterology, The Affiliated Hospital of Qingdao University, Qingdao, Shandong 266005, China

<sup>o</sup> Department of Pathology, Medical University of Vienna, Vienna 1040, Austria

<sup>p</sup> Ludwig Boltzmann Institute for Cancer Research, Vienna 1090, Austria

<sup>q</sup> Medical University of Vienna, Vienna 1040, Austria

<sup>r</sup> Institute of Animal Breeding and Genetics, University of Veterinary Medicine Vienna, Vienna 1210, Austria

<sup>s</sup> Division of Experimental Hematology, CCHMC, Cincinnati, OH 45229, USA

\* Corresponding author. 2500 Metrohealth Dr, Rammelkamp 461, Cleveland, OH 44109, USA.

E-mail address: [xxh455@case.edu](mailto:xxh455@case.edu) (X. Han).

Peer review under responsibility of Chongqing Medical University.

<sup>1</sup> Equal contribution.

Received 16 September 2022; received in revised form 22 November 2022; accepted 25 November 2022  
Available online 2 January 2023

## KEYWORDS

Cell division cycle 42 (CDC42);  
Colitis;  
Colorectal cancer (CRC);  
Inflammatory bowel diseases (IBD);  
Intestinal epithelial cell (IEC);  
Intestinal epithelial stem cell (IESC);  
Irradiation

**Abstract** CDC42 controls intestinal epithelial (IEC) stem cell (IESC) division. How aberrant CDC42 initiates intestinal inflammation or neoplasia is unclear. We utilized models of inflammatory bowel diseases (IBD), colorectal cancer, aging, and IESC injury to determine the loss of intestinal *Cdc42* upon inflammation and neoplasia. Intestinal specimens were collected to determine the levels of CDC42 in IBD or colorectal cancer. *Cdc42* floxed mice were crossed with *Villin-Cre*, *Villin-CreER<sup>T2</sup>* and/or *Lgr5-eGFP-IRES-CreER<sup>T2</sup>*, or *Bmi1-CreER<sup>T2</sup>* mice to generate *Cdc42* deficient mice. Irradiation, colitis, aging, and intestinal organoid were used to evaluate CDC42 upon mucosal inflammation, IESC/progenitor regenerative capacity, and IEC repair. Our studies revealed that increased CDC42 in colorectal cancer correlated with lower survival; in contrast, lower levels of CDC42 were found in the inflamed IBD colon. Colonic *Cdc42* depletion significantly reduced *Lgr5*<sup>+</sup> IESCs, increased progenitors' hyperplasia, and induced mucosal inflammation, which led to crypt dysplasia. Colonic *Cdc42* depletion markedly enhanced irradiation- or chemical-induced colitis. Depletion or inhibition of *Cdc42* reduced colonic *Lgr5*<sup>+</sup> IESC regeneration. In conclusion, depletion of *Cdc42* reduces the IESC regeneration and IEC repair, leading to prolonged mucosal inflammation. Constitutive monogenic loss of *Cdc42* induces mucosal inflammation, which could result in intestinal neoplasia in the context of aging. © 2023 The Authors. Publishing services by Elsevier B.V. on behalf of KeAi Communications Co., Ltd. This is an open access article under the CC BY-NC-ND license (<http://creativecommons.org/licenses/by-nc-nd/4.0/>).

## Introduction

Environmental factors, such as microbiota alterations or infection, can trigger an immune response that leads to intestinal mucosal injuries, which culminate in genetic changes and increased replication to alter intestinal epithelial stem cells (IESC) and progenitor homeostasis.<sup>1,2</sup> These changes in IESC/progenitors can break down epithelial barriers, resulting in gastrointestinal (GI) diseases, such as inflammatory bowel diseases (IBD) and colorectal cancer (CRC).<sup>3–5</sup> In North America and Europe, five million individuals are currently affected by IBD including Crohn's disease (CD) and ulcerative colitis (UC).<sup>6</sup> Chronic IBD or age-associated intestinal inflammation can directly induce the onset of CRC.<sup>7</sup> Altered IESC and progenitors play a direct role in driving chronic and relapsing mucosal inflammation in IBD to convert to colon cancer.<sup>4,5</sup> Although the mechanisms of this conversion remain enigmatic, therapeutic restoration of IESC–progenitor homeostasis is believed to improve clinical outcomes in both CD and UC patients and increase the sensitivity of colon cancers to therapies.<sup>8,9</sup>

Cell division cycle 42 (CDC42) is a small GTPase of the Rho family that establishes epithelial polarity through the PAR3-PAR6-atypical protein kinase C (aPKC) complex at the apical membrane.<sup>10</sup> Absence of CDC42 results in loss of epithelial polarity, epithelial specification, and tissue or organ formation.<sup>11</sup> Consistently, depletion of *Cdc42* impairs intestinal epithelial cell (IEC) differentiation into the functional intestinal barrier, contributing to chronic GI inflammation.<sup>12</sup> In contrast, CDC42 overexpression is associated with the development of invasive phenotypes in colon cancer.<sup>13</sup> *Cdc42* variants were recently determined as

a susceptibility locus for developing CRC.<sup>14</sup> These findings suggest that CDC42 plays a critical role in GI inflammation and tumorigenesis. However, the role of CDC42 in disease progression from chronic inflammation to colorectal cancer progression and its association with therapy have not so far been sufficiently addressed, nor was its prognostic role illuminated and targeting explored.

Intriguingly, CDC42 may be also essential for adult IESC homeostasis.<sup>15</sup> *Cdc42*-deficient IESCs lose the ability to clonally expand and differentiate, further leading to disrupted intestinal crypt–villus axis.<sup>12,15</sup> It is assumed that intestinal responses to gut injury, regeneration, and tumorigenesis are controlled by IESCs at the crypt bottom and their progenitors within the transit-amplifying (TA) zone.<sup>16</sup> IESCs were identified as *Lgr5*<sup>+</sup> and/or *Ascl2*<sup>+</sup> crypt base columnar cells (CBC) that asymmetrically divide into one new IESC and one TA cell to maintain intestinal homeostasis, or divide symmetrically into two daughter TA cells only upon tissue expansion or damage.<sup>17</sup> Interestingly, TA daughter cells can hyper-proliferate to replace injured IECs or convert into IESCs during GI injury.<sup>18</sup> The underlying mechanisms by which IESCs and daughter TA cells inter-convert upon GI injury, inflammation, and diseases are largely unclear. It has been recognized that the disturbed homeostasis from IESCs to progenitors causes intestinal neoplasia.<sup>19</sup> In this study, combining mouse injury models with patient-based observations, we investigated the role of CDC42 in the maintenance of IESCs and more rapidly proliferating progenitors during GI injury. Based on our findings, we provide a model of how IESCs respond to GI diseases and injury and suggest a potential target for direct intervention in chronic GI inflammation or inflammation-induced CRC.

## Materials and methods

### Materials

Details were listed in the **Supplemental Materials and Methods**.

### Animal resources and maintenance

The animal study protocols were approved by the Institutional Animal Care and Use Committee (IACUC) at CWRU, Cleveland, OH, USA (IACUC2021-0012), at CCHMC, Cincinnati, USA (IACUC2016-0100), and at ILAS, Beijing, China (HXN16001). Breeding pairs of *Villin-CreER<sup>T2</sup>* and *Cdc42<sup>fl/fl</sup>* mice were from CCHMC.<sup>12,20</sup> C57BL/6, *Villin-Cre*, and *Lgr5-eGFP-IRES-CreER<sup>T2</sup>* transgenic mice were purchased from Jackson Labs (Bar Harbor, MA). Constitutive or inducible depletion of *Cdc42* from IECs was achieved by breeding *Cdc42<sup>fl/fl</sup>* mice with *Villin-Cre* or *Villin-CreER<sup>T2</sup>* transgenic mice.<sup>21</sup> The inducible depletion of *Cdc42* upon *Lgr5* or *Bmi1* IESCs was investigated by crossing *Cdc42<sup>fl/fl</sup>* mice with *Lgr5-eGFP-IRES-CreER<sup>T2</sup>* or/and *Villin-CreER<sup>T2</sup>*, or *Bmi1-CreER<sup>T2</sup>* mice (JAX strain, 010,531; Fig. S1A–D).<sup>22</sup> All mice used in these studies have been backcrossed with C57BL/6 for more than ten generations and were re-genotyped with respect to *Cdc42<sup>fl/fl</sup>* and Cre prior to necropsy. All studies were performed with littermate *Cdc42<sup>fl/fl</sup>* mice designated as wild-type controls. *Cdc42<sup>fl/fl</sup>* mice with *Villin-Cre*, *Villin-CreER<sup>T2</sup>*, or *Lgr5-eGFP-IRES-CreER<sup>T2</sup>* denoted as *Vil-Cre;Cdc42<sup>fl/fl</sup>*, *VilCreER;Cdc42<sup>fl/fl</sup>*, or *Lgr5CreER;Cdc42<sup>fl/fl</sup>* mice,<sup>21</sup> were maintained under specific pathogen-free conditions in the CCHMC and ILAS Animal Care Facility.

### Biopsies and surgical specimens from IBD and CRC patients and tumor tissue microarray

CRC biopsies from 340 patients were obtained as previously described.<sup>23</sup> Tissue samples originated from specimens of patients who underwent surgical therapy of colorectal carcinoma at UICC stage II or III at the Surgical Department of the Jena University Hospital of Friedrich-Schiller University. All specimens had negative margins. Data on clinical parameters, including sex, age, tumor stage, and follow-up information, were extracted from the prospective tumor registry of the surgical clinic. Pathologic findings (*i.e.*, site of primary tumors, depth of tumor invasion, grading, lymphatic vessel invasion, venous invasion) were obtained from the pathologists' original reports.<sup>24</sup> The CRC Tissue Microarray Assay (TMA) was assembled using 0.6 mm punch biopsies from all 340 samples according to standard procedures and was described before.<sup>23,25</sup>

Colonic surgical samples from adult patients including 19 CD, 23 ileal CD, 17 UC, and 40 diagnosed colorectal adenocarcinoma patients were obtained from the University of Cincinnati Medical Center, Cincinnati, USA, division of pathology, MHMC, Cleveland, USA, and Peking Union Medical College Hospital (PUMC hospital), Beijing, China.

RNA samples of 35 cases of human IBD colonic biopsies or surgical specimens, including 10 cases of diagnosed healthy controls, 18 cases of diagnosed CD patients, and 7 cases of diagnosed UC patients were from a biospecimen bank of

Department of Gastroenterology, the Affiliated Hospital of Qingdao University, Qingdao, China. Informed consent was obtained from all of the subjects during the initial enrollment.

Prior to processing for HE, histology, RNA extraction, and patient enrollment, IRB or de-identified IRB protocols for using IBD and CRC patient samples were approved respectively by the ethics committee of Affiliated Hospital of Qingdao University, Qingdao and PUMC Hospital, Beijing, China, the local ethics committee (EC) of Jena General Hospital, Germany, and de-identified Institutional Review Board (IRB) protocols at CCHMC, Cincinnati (XH, IRB2009-1680) and MHMC/CWRU Cleveland (XH, IRB21-00237), OH, USA. All research was performed in accordance with relevant guidelines/regulations using human samples.

### Animal resources and maintenance

The animal study protocols were approved by the Institutional Animal Care and Use Committee (IACUC) at CCHMC, Cincinnati, OH, USA (IACUC2016-0100), IACUC at MHMC and CWRU, Cleveland, OH, USA (IACUC 2020–0081), and ILAS, Beijing, China (HXN16001). All mice were maintained under specific pathogen-free conditions in the CCHMC, MHMC/CWRU, and ILAS Animal Care Facility. All experiments were performed in accordance with relevant guidelines and regulations of live vertebrates. Detailed procedures for mouse crossing (Fig. S1A–D) were described in the **Supplemental Methods**.

### Radiation-induced injury models

The detailed procedure was described in the **Supplemental Methods**. The mouse numbers in each group are greater than 5 IEC or IESC *Cdc42* deficient mice.

### Animal model of colitis

Detailed method was described in the **Supplemental Methods**. The mouse numbers in each group are greater than 5 IEC or IESC *Cdc42* deficient mice.

### Immunohistochemistry (IH), immunofluorescence (IF), and immunoblotting for anti-CDC42, $\beta$ -catenin, Ki67, *Lgr5*, quantitated real-time PCR (QPCR), and TMA

Detailed methods were described in the **Supplemental Methods**.

### Enteroid and colonoid culture

Detailed culturing was described in the **Supplemental Materials and Methods**.

### Flow cytometry (FACS)

Detailed method was described in the **Supplemental Methods**.

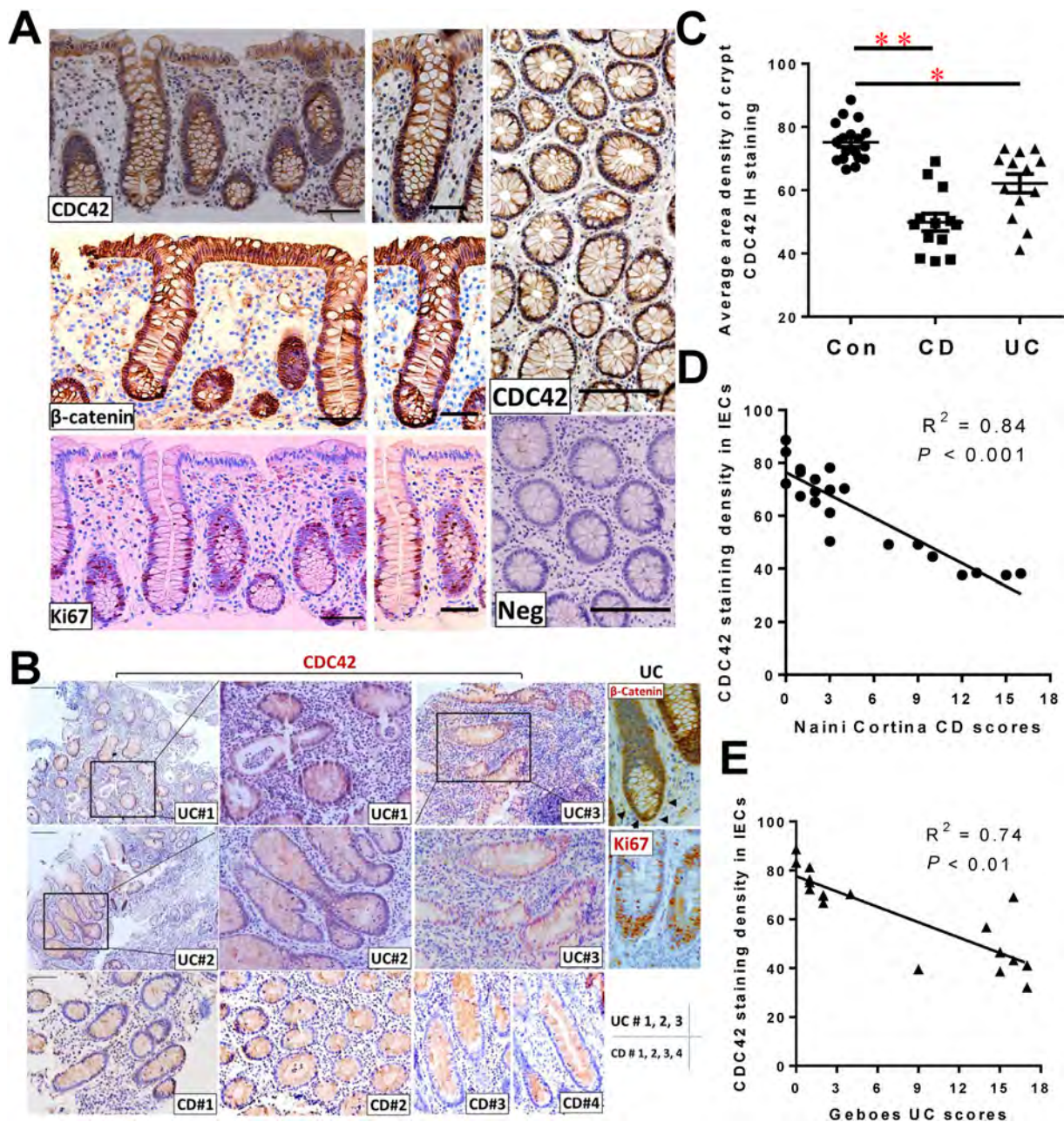


**Figure 1** Aberrant expression of CDC42 is correlated with IBD. (A, B) CDC42 expression was retrospectively investigated in colonic surgical samples in the adult CD (total 19 cases), ileal CD (23 cases), and UC (17 cases) patients were obtained from the University of Cincinnati Medical Center, Cincinnati, USA, and Peking Union Medical College Hospital (PUMC Hospital), Beijing, China. CDC42,  $\beta$ -catenin, and Ki67 expressions were examined in the colonic IECs of CD and UC samples. The area of magnified images on right is boxed in images on left. "Neg" represents a negative staining control for CDC42 antibodies. (C) The area intensity of CDC42 staining in the colonic crypts was quantified in healthy controls, CD, and UC patients. Minimal 200 crypts per group were measured.  $n > 5$  patients per group. (D, E) Linear regression analysis was used to analyze the correlation between CDC42 IH staining density with histological disease activities in UC and CD. Results are expressed as mean  $\pm$  SEM (\*\* $P < 0.01$  or \* $P < 0.05$  vs. healthy controls). Scale bars = 200  $\mu$ m.

Gamma-secretase inhibitor XX (GSI-20; DBZ; DIBENAZEPINE (S,S)-2-[2-(3,5-Difluorophenyl)acetylamino]-N-(5-methyl-6-oxo-6,7-dihydro-5H-dibenzo [b,d]azepin-7-yl) propionamide) treatment.

Detailed method was described in the **Supplemental Methods**.

### Statistical analysis

For all data compilation, the statistics software package SPSS (version 19.0) or GraphPad Prism (6.0) was used. Univariate survival analysis was subsequently carried out separately for each investigated parameter using

Kaplan–Meier estimates. Survival curves were compared and assessed using the log-rank test. *P* values of 0.05 or less were considered significant when using *t*-tests and analysis of variance (ANOVA). All statistics for colonic tissue arrays were accredited by a biostatistician of the Institute of Medical Statistics, Computer Sciences, and Documentation, Jena University Hospital.

## Results

### Aberrant expression of CDC42 is correlated with IBD

CDC42 is highly expressed in GI epithelia (Fig. 1A; Fig. S2A–C), and loss of CDC42 in the GI tract induces defective IEC proliferation and migration.<sup>12</sup> However, it is not clear if aberrant CDC42 expression regulates the GI disease course in humans or whether targeting CDC42 represents an option in gut disease. To test this hypothesis, we retrospectively investigated CDC42 expression in the colonic surgical samples obtained from adult CD (19 cases), ileal CD (23 cases), and UC (17 cases) patients obtained at the University of Cincinnati Medical Center, Cincinnati, USA, and Peking Union Medical College Hospital (PUMC Hospital), Beijing, China. CDC42 immunohistochemistry (IH) staining (Fig. 1A and B) combined with semi-quantitated pathology along with stringent negative controls showed that CDC42 expression was markedly reduced in the colonic IECs of CD samples and UC samples compared to normal patients (Fig. 1C). Interestingly, Ki67<sup>+</sup> and  $\beta$ -Catenin<sup>+</sup> crypt IECs are increased in UC samples (Fig. 1A, B). Linear regression analysis revealed that reduction in the crypt CDC42 was negatively correlated with histological disease activities in UC and CD that were determined by Geboes and global histological activity (GHA) scores,<sup>26</sup> respectively (Fig. 1D, E). To confirm the transcriptional effects of CDC42 on IECs in IBD, we enrolled healthy controls (10), CD (18), and UC (7) patients with informed consent at Qingdao University, Qingdao, China, and then performed quantitated real-time PCR (QPCR) with endoscopic biopsies. Consistently, QPCR results showed a significant reduction of CDC42 gene expression in CD and a trend toward reduction of CDC42 expression in UC (Fig. S2A). These data indicated that the reduction of crypt CDC42 expression might be associated with mucosal chronic inflammation-induced IBDs although more samples or laser capture microdissection (LCM)-captured crypts used for QPCR analysis might be required for future research.

### Aberrant expression of CDC42 is associated with CRC pathogenesis

Aberrant expression or activity of CDC42 has been reported in CRC.<sup>13</sup> To test the association of CDC42 with colonic IESCs, we utilized  $\beta$ -catenin, Ki67, and Lgr5 IH and CDC42 Tissue Microarray Assay (TMA) to retrospectively study the CDC42 in the Lgr5<sup>+</sup>,  $\beta$ -catenin<sup>+</sup>, or Ki67<sup>+</sup> colonic cancer stem cells (CSCs) from patients diagnosed with CRC. Similar to the distribution of  $\beta$ -catenin in normal colonic IECs or

IESCs, CDC42 was mainly located at the basolateral membranes of IECs and partially co-localized with Ki67<sup>+</sup> and Lgr5<sup>+</sup> colonic IESCs (Fig. 1A). To study CDC42 expression in CRC without therapeutic interventions, we collaborated with the Jena University Hospital of the Friedrich Schiller University in Jena to obtain 340 CRC specimens dating from 1993 to 2006. These patients had undergone colectomies only to remove the cancerous colonic tissues. Surgical pathologists categorized the majority of these CRC tissues as having low CDC42 expression. Histological diagnosis was established according to the guidelines of the World Health Organization.<sup>23,25</sup> Based on CDC42 immunohistochemistry staining (Fig. 2A), the 340 samples were denoted as “0” for histologically normal (0.9%, *n* = 3), “1” for mild cases (17.0%, *n* = 58), “2” for moderate (55.6%, *n* = 189) and “3” for severe (26.5%, *n* = 90) cases. TMA revealed that CDC42 expression was positively correlated with CRC disease severity (Fig. 2B). More importantly, the stronger CDC42 staining, including scores “2” and “3”, had a significant reduction in overall patient survival over the time course of five years (Fig. 2C). These data indicate that highly expressed CDC42 could be a negative prognostic marker for CRC progression and may potentially be used to determine if patients require aggressive surgery or other treatments. To test the possibility that CDC42 levels could be used as a tool for determining CRC treatment, we studied surgical specimens provided by the University of Cincinnati General Hospital in Cincinnati, PUMC Hospital in Beijing, and MHMC in Cleveland, from patients that had undergone either radiation- or chemo-therapies prior to surgical procedures. Concomitant with observations made at the Jena University Hospital, these post-treatment CRC samples showed increased CDC42,  $\beta$ -catenin, Ki67, and Lgr5 expression in the CRC area, and CDC42 staining was partially co-localized with Ki67<sup>+</sup> or Lgr5<sup>+</sup> colonic CSCs (Fig. 2D). Strikingly, we observed negligible CDC42 staining in the central cancerous areas along with less Ki67 and  $\beta$ -catenin nuclear abundance (Fig. 2D), which were reported as more differentiated cancerous cells.<sup>27</sup> In contrast, stronger CDC42 staining was found in the adjacent normal area of proliferative crypts (Fig. 2D), suggesting that CDC42 might be involved in the CRC invasive behaviors.<sup>28</sup> Our data demonstrate that aberrant expression or activity of CDC42 is associated with human GI inflammation and CRC pathogenesis. However, considering that studying the expression change in the IEC CDC42 upon treatments will need a large cohort of CRC patients, our results only provide the implication of the role of CDC42 in CRC treatment outcomes. Taken together, our data suggest that intestinal CDC42 expression could be used as a potential marker for GI chronic inflammation and implicate that CDC42 inhibition might enhance the effectiveness of CRC treatments.

### CDC42 co-localizes with Lgr5<sup>+</sup> IESCs at crypt bases

We then detected the expression of CDC42 in the mouse intestine and colon. CDC42 IH showed that it was expressed throughout intestinal and colonic IECs but was confined to the crypts including IESCs and progenitors in the TA zone (Fig. S3A, B). In Lgr5-eGFP-IRES-CreER<sup>T2</sup> (Lgr5CreER) mice,

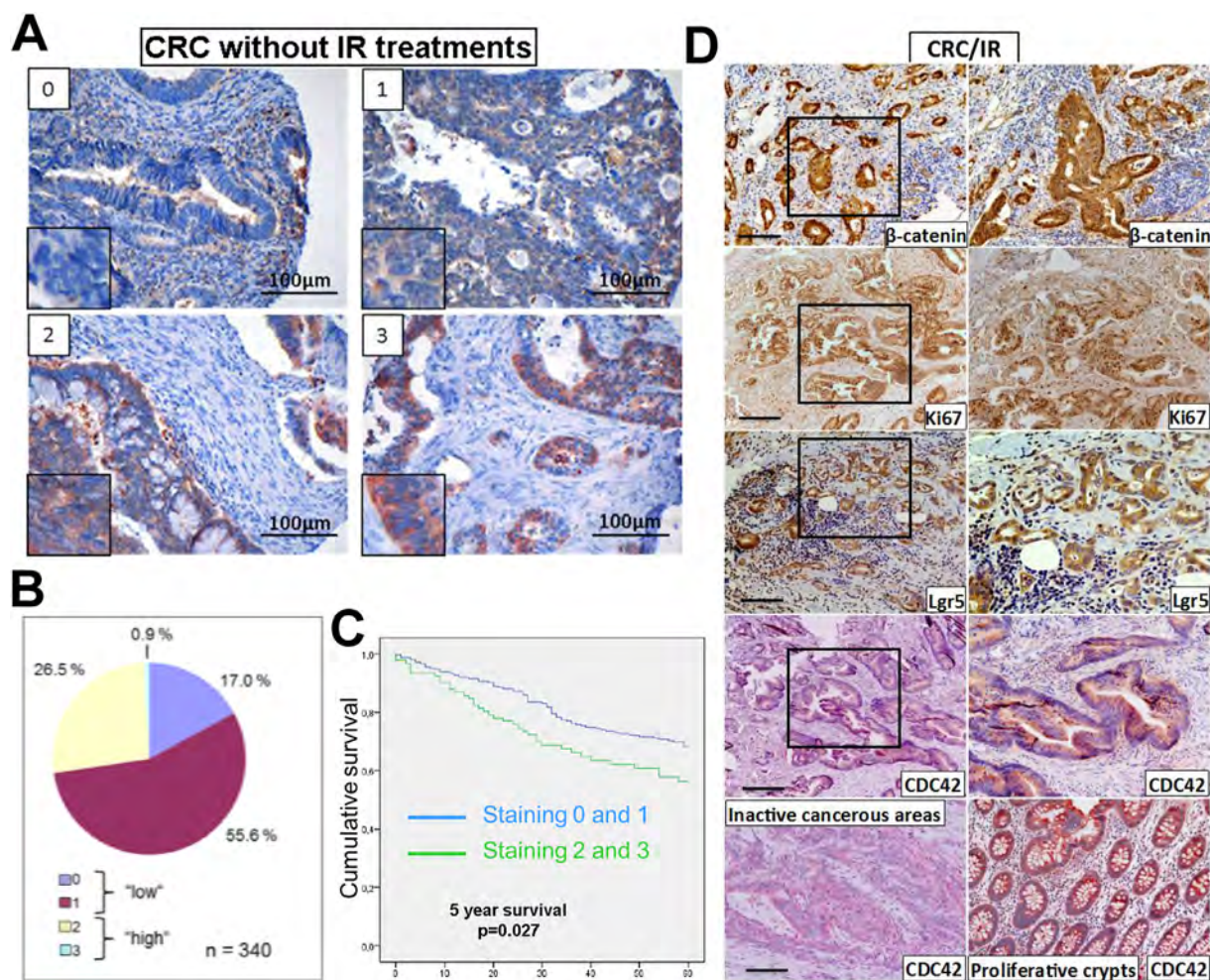


**Figure 2** Aberrant expression of CDC42 in the CRCs. (A, B) CDC42 levels were determined by IH in tissues surgically resected from 340 European CRC patients obtained between 1993 and 2006. Surgical pathologists categorized all CRC patients as either low CDC42 expression including histologically normal denoted as “0” and mild denoted as “1”, or high CDC42 expression including moderate denoted as “2” and 0.9% severe denoted as “3” (C) Patients were followed up for an overall 5 years after colectomy to determine survival, and the correlation with CDC42 staining intensity was determined. (D) CDC42 IH with surgical specimens from the University of Cincinnati Medical Center and PUMC Hospital. Representative images display  $\beta$ -catenin, Lgr5, Ki67, and CDC42 IH staining in the cancerous area, inactive cancerous areas, and proliferative crypts in CRC tissues. The area of magnified images on right is boxed in images on left. Scale bars = 200  $\mu$ m.

a Lgr5<sup>+</sup> IESC reporter mouse line, CDC42 immunofluorescence staining (IF) showed that the protein partially colocalized with the majority of Lgr5<sup>+</sup> IECs at the bases of the small intestinal and colonic crypts (Fig. S3A, B). Low levels of CDC42 were also found within surface IECs in the mouse intestine and colon stained by CDC42 IH. We then stained human CDC42 in surgical intestinal and colonic tissues. Similarly, in human intestinal and colonic tissues, we found that CDC42 was expressed in IECs and TA IECs located away from the surface IECs (Fig. 1A; Fig. S2B, 3C, 3D). Collectively, these observations suggest that CDC42 is expressed in IECs, and may play a role in IESC/progenitor in both the intestine and colon. We next tested the effects of monogenic depletion of *Cdc42* or pharmacological inhibition of CDC42 upon murine IECs.

### Constitutive depletion of intestinal *Cdc42* leads to a prolonged mucosal inflammation that induces crypt dysplasia

The intestinal villus-crypt architecture is dynamically maintained by differentiated IECs, undifferentiated IECs residing at the bottom of crypts, and differentiating progenitors in the TA zone.<sup>16</sup> Impaired homeostasis of IECs and progenitors leads to hyperplastic IEC, altered villus-crypt architecture and mucosal inflammation, and further crypt dysplasia.<sup>29</sup> To study the role of CDC42 in mucosal inflammation and dysplasia, we first crossed *Cdc42* floxed mice (*Cdc42*<sup>fl/fl</sup>) with *Villin-Cre* mice (called *VilCre*;*Cdc42*<sup>fl/fl</sup> hereinafter; Fig. 3A), by which *Cdc42* is constitutively deleted in

all IECs, including active or quiescent IESCs and their progenitors<sup>12,30</sup> (Fig. 3A). Intestinal morphology was quantified by villus length, villus width, and crypt depth, and mucosal inflammation in the 1-, 3-, 4- and 6-month-old mice. Compared to littermate controls (*Cdc42<sup>fl/fl</sup>*), *VilCre;Cdc42<sup>fl/fl</sup>* mice exhibited a disrupted villus-crypt architecture and mucosal inflammation, characterized by a significant increase in the crypt depth, villus width, and villus length and inflammatory cell infiltration (Fig. 3B, C, H). Furthermore, *VilCre;Cdc42<sup>fl/fl</sup>* mice displayed crypt dysplasia (crypt→villus hypertrophy, IEC hypertrophy and multilayers, villus fissions and “cyst” structures) (Fig. 3B, C). These morphological aberrations in the small intestines (intestine) were further

progressed in the 4- and 6-month-old mice compared to 1-month-old *Cdc42* depleted mice ( $n \geq 5$  per group,  $*P < 0.01$  vs. *Cdc42<sup>fl/fl</sup>*; Fig. 3C). Interestingly, villus length in the 6-month-old *VilCre;Cdc42<sup>fl/fl</sup>* mice was significantly shorter than 1-month-old *VilCre;Cdc42<sup>fl/fl</sup>* mice in contrast to significantly increased mucosal inflammatory cells, crypt depth and width (Fig. 3C), indicative of mucosal age-associated inflammation. These data suggest that CDC42 is required for the intestinal crypt→villus architecture and barrier formation that is maintained by the transition from IESCs to progenitors (IESCs→progenitor). Loss of CDC42 in IECs accumulates mucosal chronic inflammation, leading to crypt dysplasia.

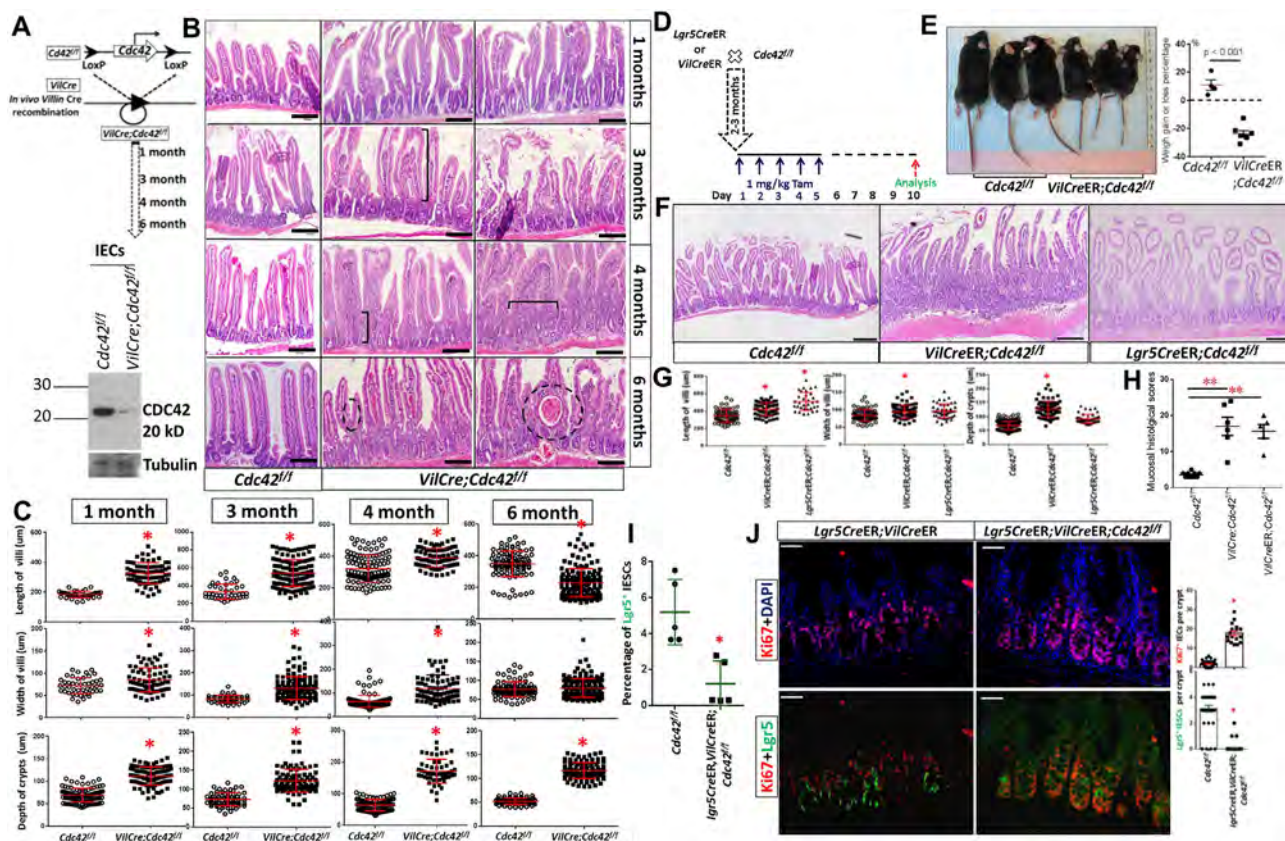


**Figure 3** Constitutive depletion of intestinal *Cdc42* leads to a prolonged mucosal inflammation that induces crypt dysplasia. (A) *Cdc42* floxed mice were crossed with *VilCre* mice to persistently delete *Cdc42* in IECs. *Cdc42* depletion was confirmed by immunoblotting of total proteins isolated from the IECs. (B) Mucosal histology was examined in 1-, 3-, 4-, and 6-month-old *VilCre;Cdc42<sup>fl/fl</sup>* mice ( $n \geq 5$  mice per group). Brackets denote villus length, villus width, and crypt depth. Unfilled circles represent villus fission and cyst structure. (C) Quantification of length and width of villi, and crypt depth in 1-, 3-, 4-, and 6-month-old *VilCre;Cdc42<sup>fl/fl</sup>* mice. Results are expressed as the mean  $\pm$  SEM ( $n \geq 5$  mice per group,  $P \leq 0.01$ ). Scale bars = 200  $\mu$ m (D) *VilCreER;Cdc42<sup>fl/fl</sup>* and *Lgr5CreER;Cdc42<sup>fl/fl</sup>* mice were given 1 mg/kg tamoxifen (Tam) intraperitoneally for five days, and then Cre-LoxP recombination for another five days to inducibly delete *Cdc42* from IECs or IESCs. (E) *VilCreER;Cdc42<sup>fl/fl</sup>* mice lost a significant amount of weight following Tam treatment. (F, G) Villus width, villus length, and crypt depth were measured in HE-stained intestines. Results are expressed as the mean  $\pm$  SEM ( $n \geq 5$  mice per group,  $*P \leq 0.01$  vs. *Cdc42<sup>fl/fl</sup>*). (H) Intestinal mucosal inflammation including IEC hyperplasia (0–3), crypt hypertrophy (0–3), crypt elongation (0–3), immune cell infiltration (0–3), and mucosal thickness, was scored in the *Cdc42<sup>fl/fl</sup>*, *VilCre;Cdc42<sup>fl/fl</sup>* (B) and *VilCreER;Cdc42<sup>fl/fl</sup>* mice (F). (I) *Lgr5<sup>hi</sup>* low, mid, and high populations of IESCs were analyzed by FACS. *Lgr5<sup>hi</sup>* populations were significantly lower in *Lgr5CreER;VilCreER;Cdc42<sup>fl/fl</sup>* mice. Results are expressed as the mean  $\pm$  SEM ( $n \geq 5$  mice per group,  $*P \leq 0.01$  vs. *Cdc42<sup>fl/fl</sup>*). (J) Intestinal tissues were isolated from *Lgr5CreER;VilCreER* or *Lgr5CreER;VilCreER;Cdc42<sup>fl/fl</sup>* mice and double stained for Ki67 (red) and/or *Lgr5* (green) by IF. The number of Ki67<sup>+</sup> IECs and *Lgr5*<sup>+</sup> IESCs per crypt was counted in 200 crypts. Results are expressed as the mean  $\pm$  SEM ( $n \geq 5$  per group,  $*P \leq 0.01$ ). Scale bars = 200  $\mu$ m.

## Inducible depletion of intestinal *Cdc42* reduces *Lgr5*<sup>+</sup> IESC numbers and increases IEC progenitor hyperplasia and mucosal inflammation, resulting in crypt dysplasia

To assess the direct role of IEC CDC42 in the IESCs → progenitor and mucosal inflammation, we crossed *Cdc42*<sup>fl/fl</sup> with *VilCreER*<sup>T2</sup> mice (called *VilCreER*;*Cdc42*<sup>fl/fl</sup> hereinafter). In these *VilCreER*;*Cdc42*<sup>fl/fl</sup> mice, depletion of *Cdc42* from IECs was induced by 5 days of tamoxifen (Tam) administration (Fig. 3D; Fig. S1B). Inducible IEC-*Cdc42* deficient mice had significantly reduced weight gain compared to controls after 5-day Tam induction and Cre recombinase (Fig. 3E). These mice also exhibited increased villus width, villus length, and crypt depth and mucosal inflammation (Fig. 3F–H) but did not develop intestinal “cyst” structures (Fig. 3F, G). We next crossed *VilCreER*;*Cdc42*<sup>fl/fl</sup> mice with *Lgr5CreER* mice (called *Lgr5CreER*;*VilCreER*;*Cdc42*<sup>fl/fl</sup> hereinafter) to study the effects of intestinal *Cdc42* depletion on *Lgr5*<sup>+</sup> IESC numbers, proliferation, and localization that affect IEC barrier formation.<sup>31</sup> *Lgr5CreER*;*VilCreER*;*Cdc42*<sup>fl/fl</sup> mice exhibited a disrupted villus-crypt architecture similar to *VilCre* or *VilCreER*;*Cdc42*<sup>fl/fl</sup> mice (Fig. 3B, F; Fig. S4A). Consistent with previous reports,<sup>12,15</sup> using GFP and lysozyme (Lyso) IF, we also found that *Lgr5*<sup>+</sup> IESCs and Paneth cells were mislocalized from intestinal crypts to villi in the *Lgr5CreER*;*VilCreER*;*Cdc42*<sup>fl/fl</sup> mice (Fig. S4A, C). *Bmi1*, a member of polycomb-repressing complex 1 (PRC1), can mark a population of quiescent IESCs that repopulates *Lgr5*<sup>+</sup> IESCs during injury.<sup>32,33</sup> To observe the role of CDC42 on other IESCs, we crossed *Cdc42*<sup>fl/fl</sup> with *Bmi1CreER*<sup>T2</sup> mice to inducibly delete CDC42 in *Bmi1*<sup>+</sup> IESCs. Compared with *VilCreER*;*Cdc42*<sup>fl/fl</sup> mice, *Cdc42* depletion in *Bmi1*<sup>+</sup> cells led to intestinal clustered dysplastic crypts and mild mucosal inflammation (Fig. S4B). Ki67:*Lgr5*-GFP double staining and fluorescence-activated cell sorting (FACS) revealed that inducible depletion of IEC *Cdc42* led to markedly reduced *Lgr5*<sup>+</sup> IESCs at the crypt bases in *VilCreER*;*Cdc42*<sup>fl/fl</sup> mice (Fig. 3I, J) in contrast to increased Ki67<sup>+</sup> IEC progenitor numbers and proliferation (Fig. 3J). These data together with histopathological analyses (Fig. 3H) suggest that progenitors undergo hyperplasia and mucosal inflammation. Taken together, our data demonstrate that loss of *Cdc42* in the different populations of IESCs disrupts *Lgr5*<sup>+</sup> IESC/progenitor homeostasis, resulting in crypt dysplasia and mucosal inflammation. CDC42 maintains the normal morphology of intestines, in part by controlling active or quiescent IESC → progenitor homeostatic proliferation.

## Inducible depletion of intestinal *Cdc42* increases $\gamma$ -irradiation-induced injury

Irradiation leads to specific injury to CBCs, which can induce enteritis and colitis.<sup>34</sup> After exposure to a high dose of irradiation, cycling CBCs undergo DNA double-strand break followed by rapid apoptosis or mitotic death, resulting in lost proliferative or regenerative capacity.<sup>31,34</sup> Depending on the irradiation dosage, progenitor pools or other IESCs replenish lost CBCs, for example, *Bmi1*<sup>+</sup> IESCs are resistant to irradiation injury and

can be activated followed by damage to the active IESCs.<sup>18,33</sup> Thus, irradiation is often utilized to test IESC/progenitor proliferative or regenerative function. To determine the role of CDC42 in the intestinal IESC/progenitor activity and IESC/progenitor function after injury, either *VilCre* or Tam-inducible *VilCreER* recombination was used to constitutively or inducibly delete *Cdc42* in IECs. *VilCre* and *VilCreER*;*Cdc42*<sup>fl/fl</sup> mice were then irradiated (Fig. 4A). Constitutive depletion of *Cdc42* in IECs significantly reduced the number of regenerated crypts 3 days post-irradiation in comparison with littermate controls (Fig. 4B). Consistently, inducible depletion of *Cdc42* showed significantly reduced the number of regenerated crypts compared to controls ( $0.6 \pm 0.1$  crypts per mm in *VilCreER*;*Cdc42*<sup>fl/fl</sup> versus  $13.5 \pm 0.5$  per mm in *Cdc42*<sup>fl/fl</sup> mice,  $n = 3$ , \* $P < 0.01$ ; Fig. 4B, C). Both *VilCre*;*Cdc42*<sup>fl/fl</sup> and *VilCreER*;*Cdc42*<sup>fl/fl</sup> mice exhibited significantly worse mucosal injury post-irradiation (Fig. 4B, C). These data indicate that CDC42 is required for IESC/progenitor regeneration; in turn, loss of CDC42 deteriorates mucosal healing. By crossing *Lgr5CreER* with *Cdc42*<sup>fl/fl</sup> mice, *Cdc42* can be depleted in IESCs in a mosaic fashion.<sup>35</sup> Interestingly, we found that depletion of *Cdc42* led to reduced bromodeoxyuridine (BrdU) incorporation into IECs in the regenerated crypts following irradiation.

Paneth cells are located at the bottom of crypts, playing a niche role in protecting IESC self-renewal and proliferation. Loss of Paneth cell niches leads to reduced *Lgr5*<sup>+</sup> IESC numbers.<sup>36</sup> Intriguingly, Paneth cell precursors are postulated to represent dormant IESCs that can be reactivated after injury to become *Lgr5*<sup>+</sup> IESCs.<sup>37</sup> Previous work has demonstrated that CDC42 controls Paneth cell migration and maturation.<sup>15</sup> Consistently, utilizing 12-Gy irradiation injury, we found that inducible depletion of *Cdc42* caused significantly increased Paneth cell migration and reduced numbers of niche Paneth cells at the regenerated crypts (Fig. 4D–F). Similarly, *LgrCreER*;*Cdc42*<sup>fl/fl</sup> mice exhibited significant Paneth cell migration to the villus surface in the irradiation-treated mice compared to control mice (Fig. 4D, F; Fig. S4C), but did not show reduced numbers of Paneth cells at the crypt base (Fig. 4D, E). In addition, dysfunctional or misallocated Paneth cells can be the site of origin for intestinal inflammation.<sup>38</sup> Therefore, our also data suggest that IEC CDC42 might have a role in maintaining the Paneth cell niche. Loss of *Cdc42* could impair Paneth cell maturation to control mucosal inflammation.

## Depletion of colonic *Cdc42* leads to transformed colonic IECs sensitive to irradiation-induced colitis

Aging is considered to be a GI stressor and is directly associated with senescence-associated mucosal inflammation and IEC transformation.<sup>29,39</sup> In addition, CDC42 has been reported to suppress the metastasis of intestinal tumors and mutant *Cdc42* has been identified as a risk factor for colorectal cancer.<sup>40</sup> To determine if loss of *Cdc42* is sufficient to alter IEC transformation in aged mice, we examined colon morphology in 9- to 13-month-old *VilCre*;*Cdc42*<sup>fl/fl</sup> mice devoid of CDC42 (Fig. 5A). We found that persistent depletion of *Cdc42* in the colon led to colonic IEC hyperplasia, mucosal inflammation, and sporadic



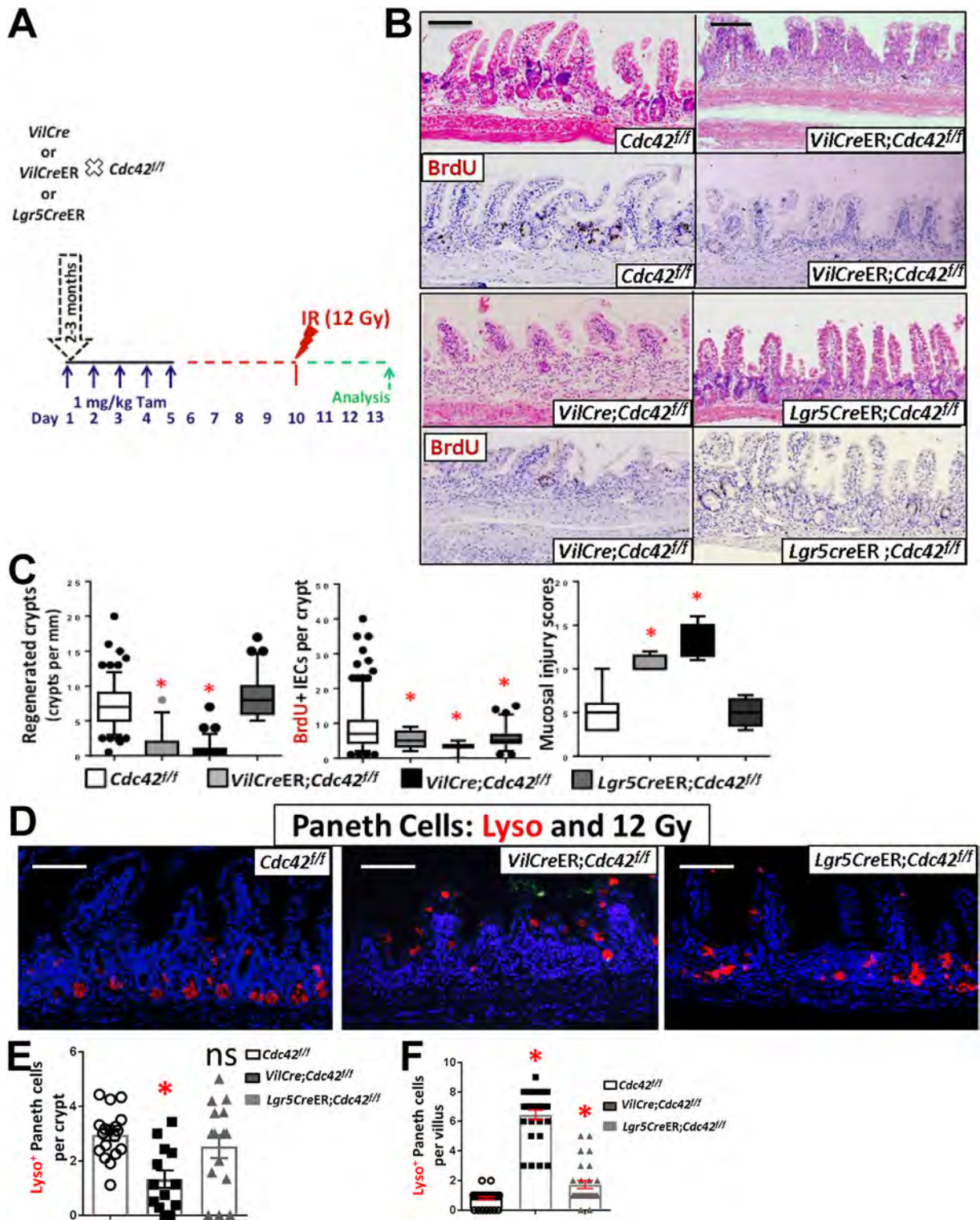


**Figure 4** Inducible depletion of intestinal *Cdc42* increases  $\gamma$ -irradiation-induced injury. **(A)** *VilCreER;Cdc42<sup>fl/fl</sup>* and *Lgr5CreER;Cdc42<sup>fl/fl</sup>* mice were given 1 mg/kg Tam for five days, 10 min of 12 Gy irradiation following five-day Cre recombination after the last Tam injection, and then sacrificed three days post-irradiation **(B, C)** Crypt regeneration was quantified by counting regenerated mucosal crypts and BrdU staining. The intestinal mucosal injury was determined by histological scores. Results are expressed as the mean  $\pm$  SEM ( $n = 6$  or 7 mice per group,  $*P \leq 0.01$ ). **(D–F)** Paneth cells were identified by lysozyme (Lyso) IF. Lyso<sup>+</sup> Paneth cells were counted within crypts and on the surface of villi. Results are expressed as the mean  $\pm$  SEM ( $n = 6–7$  mice per group, a total of 200 crypts per group,  $*P \leq 0.01$ ). Scale bars = 200  $\mu$ m.

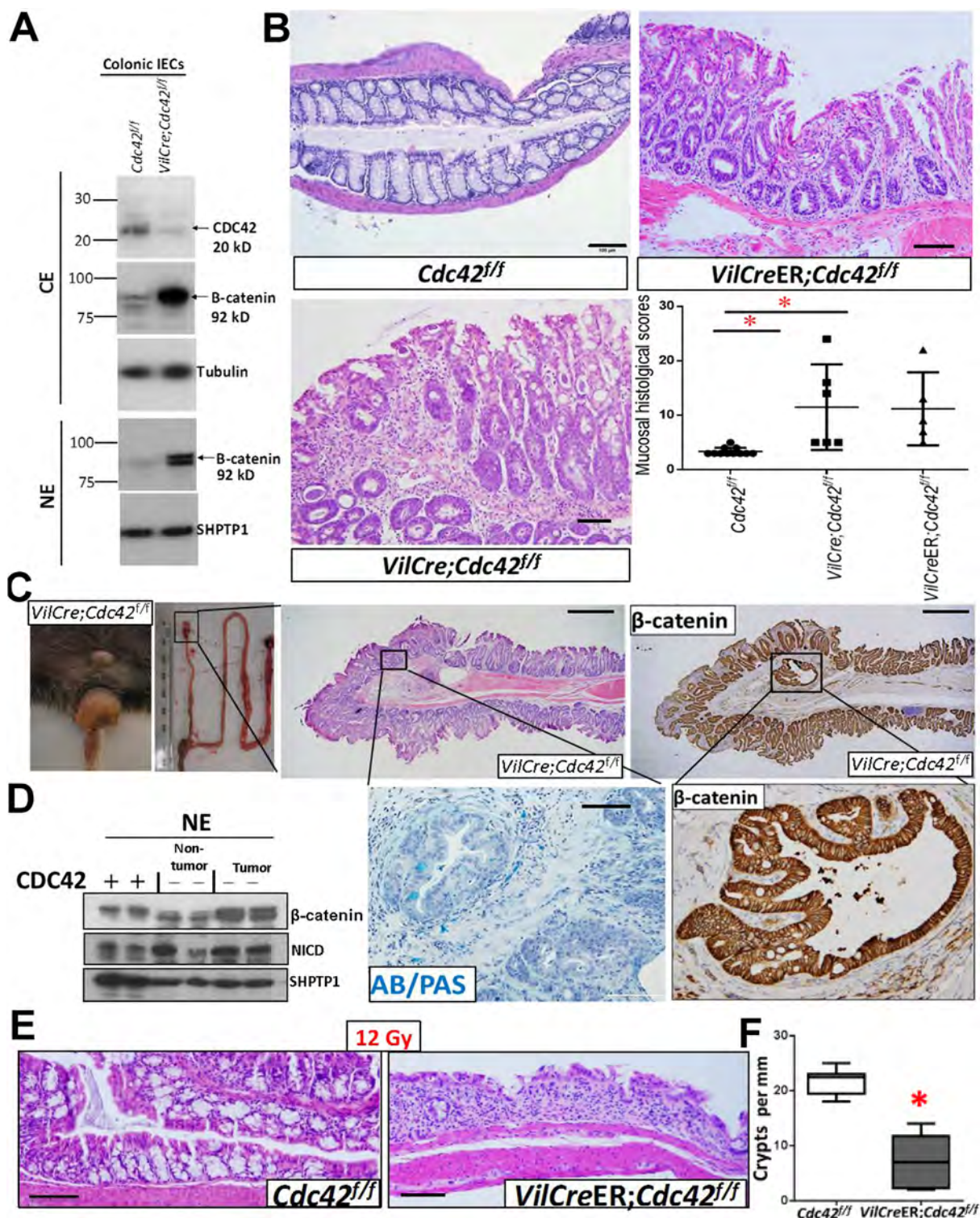


**Figure 5** Depletion of colonic *Cdc42* leads to transformed colonic IECs sensitive to irradiation-induced colitis. **(A)** Colonic IECs were isolated for extracting cytosolic and nuclear proteins (CE and NE). CDC42 expression was determined in CE and β-catenin was determined in NE by immunoblotting.  $n = 3$  mice per group. **(B)** Colonic histology in 5-month-old *VilCre;Cdc42<sup>f/f</sup>*, *VilCreER;Cdc42<sup>f/f</sup>*, and *Lgr5CreER;Cdc42<sup>f/f</sup>* mice were determined by HE staining. The number of aberrant crypt foci (ACF) was counted. Colonic mucosal inflammation including IEC hyperplasia, crypt elongation, crypt hypertrophy, crypt elongation, immune cell infiltration, mucosal thickness, ACF, mucin-depleted foci (MDF) was scored in the *Cdc42<sup>f/f</sup>*, *VilCre;Cdc42<sup>f/f</sup>* and *VilCreER;Cdc42<sup>f/f</sup>* mice. Results are expressed as the mean  $\pm$  SEM ( $n \geq 5$  mice per group,  $*P \leq 0.05$  vs. *Cdc42<sup>f/f</sup>*). **(C)** Gross lesions were shown in the colorectal area, MDF was shown by Alcian Blue/Periodic Acid Schiff (AB/PAS) staining, and β-catenin was detected by IH. Areas of magnified images underneath are boxed in images.  $n = 6-7$  mice per group. **(D)** β-catenin expression was detected in the NE of the colon by immunoblotting. **(E, F)** *VilCreER;Cdc42<sup>f/f</sup>* mice were exposed to 12 Gy irradiation. Colonic histology (E) and regenerated crypts (F) were quantified 3 days post-irradiation ( $n \geq 5$ ,  $*P \leq 0.01$ ). Scale bars = 100  $\mu$ m.

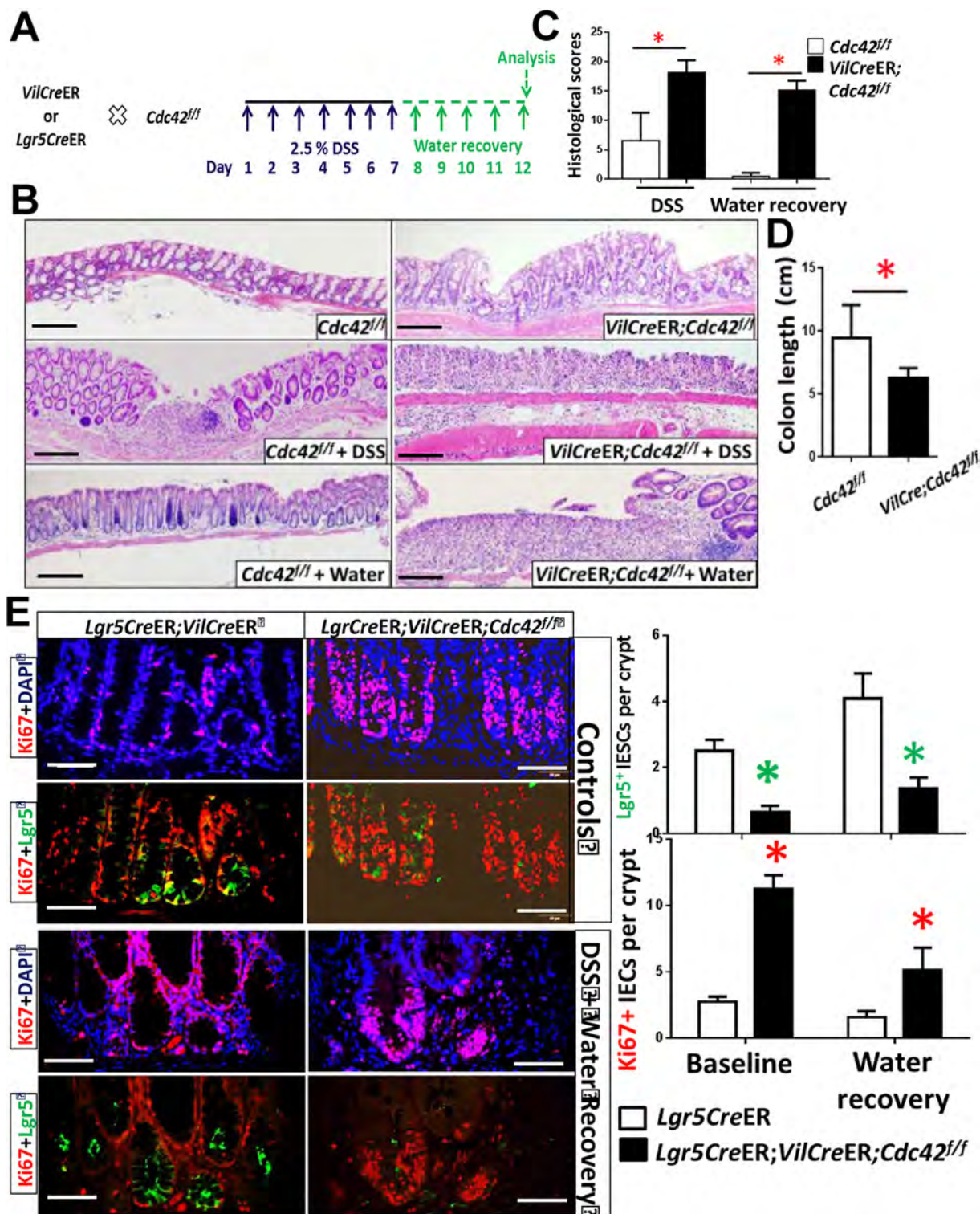


**Figure 6** Depletion of *Cdc42* reduces colonic IESC repair, resulting in the susceptibility to colitis. (A) After five days of Tam-induced Cre recombination, *VilCreER;Cdc42<sup>fl/fl</sup>* and *Lgr5CreER;Cdc42<sup>fl/fl</sup>* mice were exposed to 2.5% DSS in the water for seven days or five days of DSS plus water recovery for five days (B–D) Colonic mucosal histology and colon length were quantified after DSS treatment for seven days ( $n \geq 5$  mice per group,  $*P \leq 0.01$ ) (E) *Lgr5CreER;VilCreER;Cdc42<sup>fl/fl</sup>* mice were treated for seven days with DSS followed by five days of water recovery. Ki67<sup>+</sup> (red) or Lgr5<sup>+</sup> (green) IECs were identified and semi-quantified. Results are expressed as the mean  $\pm$  SEM ( $n \geq 5$  mice per group,  $*P \leq 0.01$ ). Scale bars = 200  $\mu$ m.

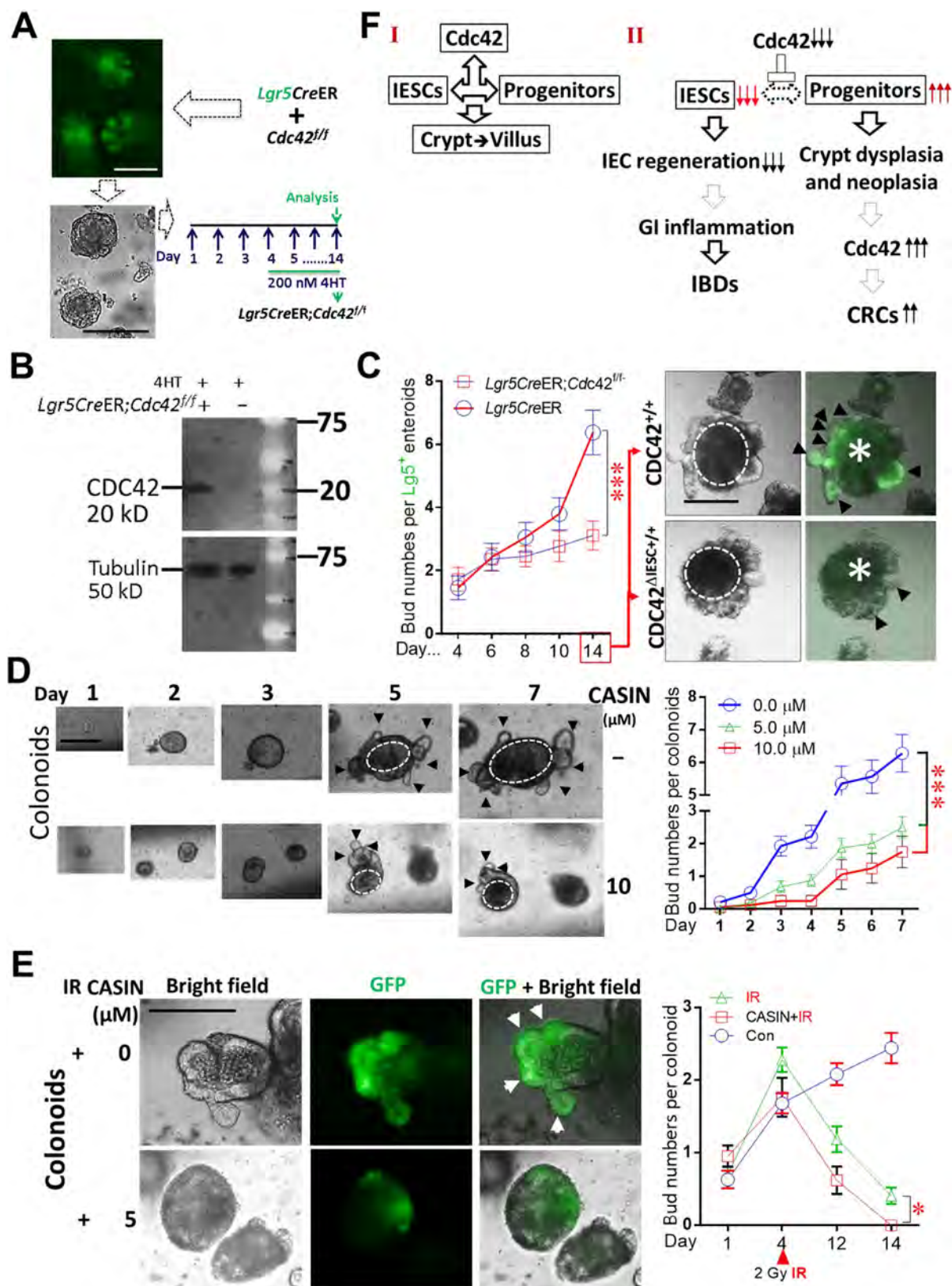


**Figure 7** Genetic depletion or pharmacological inhibition of CDC42 sensitized IESCs to injury. (A) Intestinal crypts were isolated from *Lgr5CreER;Cdc42<sup>fl/fl</sup>* mice, and resuspended in Matrigel with epidermal growth factor (EGF), Noggin, and R-spondin for culture from day 1 through day 4. *Cdc42* depletion was induced by 200 nM 4HT in the enteroids or *Lgr5<sup>+</sup>* enteroids. Enteroids were cultured in six parallel wells per mouse for each experiment ( $n = 4$  mice per group). The number of crypt buds was counted daily in a minimum of 10 enteroids per well after 4HT-induced *Cdc42* depletion. (B) Immunoblotting showed the efficiency of *CDC42*

macroadenoma displaying colorectal polyps, distorted or serrated crypts, mucin-depleted foci (Fig. 5B, C; Fig. S5A). Importantly, persistent depletion of *Cdc42* in IECs led to colorectal adenoma, which was displayed in 7 out of 9 mice and characterized by aberrant crypt foci (ACF) and clustered mucin-depleted foci (MDF), strongly indicating the role of *Cdc42* in the intestinal neoplasia (Fig. 5C, inserts). Immunoblotting showed that  $\beta$ -catenin nuclear abundance was increased in the crypt in the tumor area compared to the normal colonic or intestinal mucosa in the mutant mice, in which  $\beta$ -catenin was confined mainly between cell boundaries (Fig. 5A, C, D; Fig. S5B). The increased nuclear abundance of  $\beta$ -catenin in the dysplastic crypt IECs might be upon *Lgr5*<sup>+</sup> cell loss in the context of aging. Interestingly, colonic NICD1 expression, which was used to indicate the activation of intestinal Notch signaling,<sup>41</sup> was not different between the colonic normal area and tumor area (Fig. 5D). Consistently, inducible depletion of *Cdc42* in colonic IECs displayed microadenoma with ACF and acute inflammation with severe inflammatory cell infiltration (Fig. 5B and Supplementary Materials, arrows in Fig. S5A). We next exposed inducible IEC *Cdc42*-deficient mice to irradiation injury and examined the regeneration of *Cdc42*<sup>-/-</sup> IECs. We found the limited regeneration of nascent crypts in the colon 3 days post-irradiation and severe IR-induced colitis (Fig. 5E, F), strongly suggesting that loss of *Cdc42* in IECs reduced IESC regeneration and colonic IEC repair, further increased accumulation of mutation. These data indicate that mutant *Cdc42* plays an important role in colonic IEC transformation in the aged colon due to accumulated mucosal inflammation, and susceptibility to injury. Taken together, loss of CDC42 might accumulate colonic IEC mutations to induce spontaneous intestinal inflammation, which causes colitis and high-grade crypt dysplasia. We next investigated the requirement of CDC42 against colonic inflammation.

### Depletion of *Cdc42* reduces colonic IESC repair, resulting in the susceptibility to colitis

To study the requirement of CDC42 for controlling colonic inflammation to develop as colitis, IEC CDC42 was inducibly deleted in mice and were then challenged with 2.5% dextran sulfate sodium (DSS) for seven days, which is known to induce colitis in mice<sup>30</sup> (Fig. 6A; Fig. S1B). Following 7 days of DSS treatment, the colitis was more severe in the inducible *Cdc42*-deficient mice than in controls, which is consistent with the above observations that lack of CDC42 leads to irradiation colitis. To determine if the colitis could be healed, we allowed five days of recovery after DSS

treatment. Following this recovery period, *Cdc42*-deficient mice displayed increased mucosal injury and shorter colon length compared to controls (Fig. 6B–D), indicating that *Cdc42*-deficient colonic IESCs can reduce the mucosal regenerative and healing capacity. To further test the effects of CDC42 upon colonic IESC regeneration, we exposed *Lgr5CreER;VilCreER;Cdc42<sup>fl/fl</sup>* mice to the colitis induction and healing paradigm. We found reduced numbers of *Lgr5*<sup>+</sup> colonic IESCs in the *Cdc42*-deficient mice and delayed *Lgr5*<sup>+</sup> IESC recovery following DSS treatment (Fig. 6E). Conversely, colonic progenitors and IECs displayed a remarkable hyperplastic proliferation in *Cdc42*-deficient IECs compared to controls, as indicated by Ki67 staining (Fig. 6E). Together, these data suggest that CDC42 is required for colonic *Lgr5*<sup>+</sup> IESC regeneration. Loss of CDC42 leads to reduced regenerative capacity (IESC → progenitor) that impairs mucosal healing and induces colitis, indicating that CDC42 is a protective factor against colonic injury. Our results also suggest that the dysplastic crypt lesions are secondary to colonic chronic inflammation induced by lack of IEC *Cdc42*.

### Inducible depletion or pharmacological inhibition of CDC42 leads to impaired IESC capacity for crypt formation and sensitizes IESCs to irradiation injury

An intact crypt or single *Lgr5*<sup>+</sup> IESC can generate ever-growing, self-organizing “mini-guts” with a defined crypt–villus axis,<sup>42</sup> which is a great *in vitro* model to study the regenerative capacity of IESCs and progenitors after injury or crypt formation capacity during various insults.<sup>43</sup> We isolated and cultured IESCs from *Lgr5CreER;Cdc42<sup>fl/fl</sup>* or *VilCreER;Cdc42<sup>fl/fl</sup>* mice (Fig. 7A). By adding 4-hydroxy-tamoxifen (4HT) to culture media, *Cdc42* was inducibly deleted in *Lgr5*<sup>+</sup> IESCs<sup>44</sup> (Fig. 7B). *Lgr5*-GFP<sup>+</sup> crypts and crypt formation of enteroids were used to evaluate the effects of CDC42 upon the IESC proliferative capacity. The clonogenic analysis demonstrated that inducible depletion of *Cdc42* from *Lgr5*<sup>+</sup> IESCs resulted in markedly reduced enteroid formation and *Lgr5*-GFP<sup>+</sup> IESC proliferation in a time-dependent manner (Fig. 7C). To confirm the genetic depletion data, we utilized CASIN, a selective CDC42 activity inhibitor,<sup>45</sup> to partially block GTPase function in the enteroids. Consistently, CASIN at 10  $\mu$ M significantly reduced enteroid budding (Fig. 7D). *Cdc42* variants were identified as genetic risk factors of CRC, but functional genetic proof had so far not been performed.<sup>14</sup> In line with the important role of CDC42 as a key protein during colon crypt regeneration and in counteracting inflammation-induced colitis, we found that

depletion (C) Results are expressed as a graph of crypt buds per crypt or as the number of crypt buds versus time (days). One-way ANOVA was used to test for the variance of two groups (\* $P < 0.01$ ). Representative enteroids over time are shown. (D) 2-[(2,3,4,9-Tetrahydro-6-phenyl-1*H*-carbazol-1-yl)amino]ethanol (CASIN), a selective CDC42 GTPase inhibitor, was used to partially block CDC42 signaling in the enteroids. CASIN at 5 or 10  $\mu$ M significantly reduced enteroid budding. Representative enteroids are shown, from which budding curves were created. (E) Colonoids from colonic crypts were cultured and passaged into six parallel wells per mouse for each experiment ( $n = 4$  mice per group). The colonoids were then exposed to 2 Gy irradiation in the absence or presence of 5  $\mu$ M CASIN. Representative colonoids are shown. The number of crypt buds was counted daily for a minimum of 10 colonoids per well after CASIN-induced CDC42 inhibition. CASIN further reduced the number of crypt buds after irradiation. Scale bars = 200  $\mu$ m. (F) Proposed model for CDC42 requirement in maintaining IESC and progenitor homeostasis (I); loss of CDC42 leads to susceptibility to GI diseases and aberrantly increased CDC42 promotes CRC progression (II).

*Cdc42* depletion induced colon cancer phenotypes that were more vulnerable to irradiation injury (Fig. 5E). Thus, *Lgr5*<sup>+</sup> intact colonic crypts were isolated and colonoids derived from colonic crypts were grown to determine whether pharmacological inhibition of CDC42 would sensitize colonic IESCs to irradiation. We subjected wild-type colonoids to 2 Gy  $\gamma$ -irradiation. We determined that after irradiation, all colonoids lost some proliferative capacity (Fig. 7E), but CASIN-treated colonoids showed significantly reduced budding compared to irradiation-treated control colonoids (Fig. 7E). Taken together, our *in vitro* experiments demonstrate that reduced CDC42 impairs crypt formation and sensitizes the colonic IECs to noxae that predispose to colitis and CRC development.

## Discussion

The analysis of a cohort of colorectal cancer patients showed that high expression of CDC42 was a negative prognostic marker but was associated with good prognosis in chronic inflammatory diseases, such as IBD, arguing for a contradictory role of CDC42 in chronic inflammation in benign versus progressed colon neoplasia. In this article, we utilized unique mouse models of GI injury and state-of-the-art murine organoid cultures to show that CDC42 is essential for maintaining IESC  $\rightarrow$  progenitor homeostasis and regenerative response to intestinal or colonic injuries (Fig. 7F–I), including colitis and tumorigenesis. Monogenic loss of CDC42 fails intestinal IESC regeneration and repair of the impaired IEC barriers that sequentially induce mucosal inflammation, which is known to play a causal role in intestinal crypt dysplasia in the context of aging that might result in CRC. We conclude that lack of intestinal CDC42 disrupts the homeostatic transition of IESCs to progenitors, leading to impaired IEC regeneration that induces GI mucosal inflammation, which is susceptible to colitis. In turn, the disrupted transition from IESCs to progenitors leads to aberrantly activated progenitor proliferation, crypt dysplasia and neoplasia along with increased CDC42 expression, which could promote colon cancer development or CAC progression (Fig. 7F–II).

CDC42 is classified into the Rho family of GTPases along with Rac 1 and RhoA, a family that is highly conserved in regulating epithelial morphogenesis, apicobasal polarity, and intercellular junction remodeling during development.<sup>45–47</sup> CDC42 signaling is switched “on” or “off” by its intrinsic GTPase activity between an inactive GDP-bound state and an active GTP-bound state to regulate various essential cellular processes during homeostases, such as cell cycling, migration, and fate determination.<sup>48</sup> Several studies reported that *Cdc42* mRNA expression or CDC42 kinase activity is increased in colorectal adenocarcinoma<sup>13,49</sup> and inhibition of CDC42 suppresses primary colon cancer growth in mice.<sup>50</sup> Conversely, deletion or reduction of CDC42 promotes epithelial hyperplasia and tumorigenesis in the liver and skin by disturbing  $\beta$ -catenin degradation.<sup>51,52</sup> These data suggest that epithelial CDC42 signaling has a dual role in the pro-oncogenic transformation and tumor suppression depending on downstream effectors and co-factors. Our murine data suggest that CDC42 is essential for protecting

IESCs from intestinal injury and for preventing colonic IEC transformation into colorectal cancer. Because only scarce information exists on expression and activation levels of CDC42 in chronic inflammatory disease of the gut and associated colorectal cancer manifestation and progression, we undertook a detailed comparative pathology study. We found that CDC42 loss and low expression correlate with increased survival in colorectal cancer patients.

Aging or colitis can promote chronic intestinal inflammation to induce colorectal cancer, which involves multiple oncogenic pathways in IECs, such as *APC*<sup>min</sup>, *KRAS*, and *p53*.<sup>29,53–56</sup> Sequential accumulation of activating and inactivating mutations in various oncogenes and tumor suppressors could drive the transition from normal IESCs at the crypt bottom to CSCs that lead to CRC.<sup>19,53,57</sup> Consistent with previous reports,<sup>12</sup> our results showed that depletion of *Cdc42* in IECs led to IESC progenitor hyperplastic proliferation and IEC dysplasia, and mucosal inflammation in the context of aging. In contrast, numbers of *Lgr5*<sup>+</sup> IESCs as well as activity in response to irradiation injury were significantly reduced by either inducible or persistent depletion of IEC CDC42. Strikingly, we observed that depletion of *Cdc42* led to intestinal senescence-associated secretory phenotypes (Fig. S4C), and colonic neoplasia that developed as macroscopic adenomas located in the colorectal area after 9–13 months. These new findings suggest that a single mutation of *Cdc42* might induce colonic neoplasia when combined with other stress factors, such as aging and chronic injuries. However, the loss of *Cdc42* led to an increased crypt cell death, which most likely induced a compensatory proliferation from the TA population. Intriguingly, mice with loss of colonic *Cdc42* were more susceptible to colitic injury with decreased colonic *Lgr5*<sup>+</sup> IESC regeneration and delayed mucosal healing. Furthermore, genetic or pharmacological inhibition of CDC42 impaired colonoid regeneration. Our data suggest that on the one hand, CDC42 is required for IESC homeostatic proliferation towards progenitors, and thus indispensable for colonic mucosal repair. On the other hand, loss of CDC42 may increase sensitivity to intestinal injury, which could be the cause of IBD susceptibility.

Interestingly, using *Olfm4CreER*<sup>T2</sup>, a recent study showed that depletion of *Cdc42* leads to the disrupted apical-basal polarity in the IEC compartment and crypt hyperproliferation.<sup>58</sup> However, *Olfm4* marks the small intestinal IESCs as well as their progenitors, and *Olfm4*-driven GFPCreER<sup>T2</sup> expression induces the depletion of *Cdc42* in both small intestinal IESCs and progenitors in TA zone.<sup>59</sup> In contrast, *Lgr5* marks the small intestinal and large crypt IESCs, and *Lgr5*-driven CreER<sup>T2</sup> expression induces the depletion of *Cdc42* in the small and large intestinal IESCs.<sup>60</sup> Therefore, our data not only reflect the enteropathy in small intestines due to defective CDC42 but also provided evidence of CDC42 requirement to large bowels, where inflammation and neoplasia often occurred. Our future research might focus on whether CDC42 or *Cdc42* status in IBD patients or aged subjects is correlated with chronic mucosal inflammation and progression to CRC.

Wnt and Notch signaling pathways regulate IEC homeostasis and differentiation.<sup>61</sup> Constitutive activation of a Wnt target gene drives the formation of intestinal benign

adenomas<sup>57,62</sup>; by contrast, inhibition of Notch promotes IESC expansion towards a secretory fate to maintain the undifferentiated state in *Apc*-mutant neoplastic IECs.<sup>63</sup> Our data showed that depletion of *Cdc42* increased  $\beta$ -catenin nuclear abundance in the transformed colonic IECs, but the  $\beta$ -catenin expression did not display a significant alteration in the normal area of *Cdc42*-deficient colon or small intestines. Coincidentally, the adenoma in the *Cdc42*-deficient mice lacked mucin, indicating that depletion of *Cdc42* led to the loss of *APC* and activation of  $\beta$ -catenin.<sup>57</sup> These data suggest that IEC CDC42 could be a neoplastic marker. In contrast, depletion of *Cdc42* leads to increased NICD1 expression in intestinal IECs and mislocalized Paneth cells, which is often senescence-associated intestinal inflammation (Fig. S6A). These data indicate an activated Notch signaling after depleting *Cdc42*, which might alter Paneth cell maturation. Although depletion of colonic *Cdc42* did not change NICD1 in the colon, *Cdc42*-depleted mice that were challenged by  $\gamma$ -secretase for 5 days, a Notch inhibitor, displayed ameliorated mucosal hyperplastic lesions in the small intestine (Fig. S6B). Nevertheless, these data suggest that loss of CDC42 function might differentially affect intestinal and colonic IESC/progenitors. In future research, we will use unbiased RNA sequencing to determine the transcriptional effects of CDC42 signaling upon both the Wnt and Notch pathways.

Clinical therapeutics targeting CSCs are being developed for CRC treatment.<sup>64</sup> CDC42 is newly identified as a cancer marker and is highly expressed in metastatic tumors.<sup>13</sup> Interestingly, our data showed that CASIN, a CDC42 GTPase inhibitor induced the loss of proliferation in the cultured colonoids post-irradiation. This finding was consistent with our murine data showing that intestinal and colonic IESCs lacking CDC42 are highly sensitive to irradiation injury. These data further suggest that high or low CDC42 expression could be relevant as a protein marker that indicates inflammatory response outcome upon irradiation treatment of CRC. Our studies are highly relevant to the pathogenesis of CRC in the setting of aging or colitis.

In summary, we utilized unique mouse models, human samples, and murine organoid culture with loss of CDC42 function to define a potential marker reflecting intestinal injury and CSC treatment outcomes. Therefore, our results present a novel therapeutic direction for CRC.

## Conclusions

Depletion of *Cdc42* disrupts the IESC transition to active progenitors. Monogenic loss of *Cdc42* initiates intestinal neoplasia, leading to colorectal adenoma in the context of aging.

## Author contributions

XH contributed to the study concept and design. XH, DZ, WT, HN, MS, TK, FK, MT, LD, and WT contributed to data acquisition. XH and YZ generated transgenic mice. XH, RM, YZ, HR, HD, TK, FK, JW, LK, and WT analyzed the data. YZ, RM, LK, FK, and HD contributed reagents/materials/analysis tools. XH wrote the manuscript.

## Conflict of interests

All authors have no conflicting financial or non-financial interests.

## Acknowledgements

This work was supported by NIDDK R01, USA (No. R01DK123299) (X.H.) and MHMC/CWRU start-up (X.H.). R.M. was supported by a private cancer metabolism grant donation from Liechtenstein and the Austrian Science Fund (FWF) (No. SFB F4707 and SFB-F06105).

## Appendix A. Supplementary data

Supplementary data to this article can be found online at <https://doi.org/10.1016/j.gendis.2022.11.024>.

## References

- Hirayama K, Itoh K. Human flora-associated (HFA) animals as a model for studying the role of intestinal flora in human health and disease. *Curr Issues Intest Microbiol*. 2005;6(2):69–75.
- Shah SC, Itzkowitz SH. Colorectal cancer in inflammatory bowel disease: mechanisms and management. *Gastroenterology*. 2022;162(3):715–730.
- Bouma G, Strober W. The immunological and genetic basis of inflammatory bowel disease. *Nat Rev Immunol*. 2003;3(7):521–533.
- He XC, Yin T, Grindley JC, et al. PTEN-deficient intestinal stem cells initiate intestinal polyposis. *Nat Genet*. 2007;39(2):189–198.
- Quante M, Wang TC. Stem cells in gastroenterology and hepatology. *Nat Rev Gastroenterol Hepatol*. 2009;6(12):724–737.
- Hanauer SB. Inflammatory bowel disease: epidemiology, pathogenesis, and therapeutic opportunities. *Inflamm Bowel Dis*. 2006;12(Suppl 1):S3–S9.
- Farraye FA, Odze RD, Eaden J, et al. AGA technical review on the diagnosis and management of colorectal neoplasia in inflammatory bowel disease. *Gastroenterology*. 2010;138(2):746–774.
- Dekaney CM, Rodriguez JM, Graul MC, et al. Isolation and characterization of a putative intestinal stem cell fraction from mouse jejunum. *Gastroenterology*. 2005;129(5):1567–1580.
- Spence JR, Mayhew CN, Rankin SA, et al. Directed differentiation of human pluripotent stem cells into intestinal tissue *in vitro*. *Nature*. 2011;470(7332):105–109.
- Lin D, Edwards AS, Fawcett JP, et al. A mammalian PAR-3-PAR-6 complex implicated in Cdc 42/Rac 1 and aPKC signalling and cell polarity. *Nat Cell Biol*. 2000;2(8):540–547.
- Kesavan G, Sand FW, Greiner TU, et al. Cdc42-mediated tubulogenesis controls cell specification. *Cell*. 2009;139(4):791–801.
- Melendez J, Liu M, Sampson L, et al. Cdc42 coordinates proliferation, polarity, migration, and differentiation of small intestinal epithelial cells in mice. *Gastroenterology*. 2013;145(4):808–819.
- Gómez Del Pulgar T, Valdés-Mora F, Bandrés E, et al. Cdc42 is highly expressed in colorectal adenocarcinoma and down-regulates ID4 through an epigenetic mechanism. *Int J Oncol*. 2008;33(1):185–193.
- Al-Tassan NA, Whiffin N, Hosking FJ, et al. A new GWAS and meta-analysis with 1000 Genomes imputation identifies novel risk variants for colorectal cancer. *Sci Rep*. 2015;5:10442.

15. Sakamori R, Das S, Yu S, et al. Cdc42 and Rab8a are critical for intestinal stem cell division, survival, and differentiation in mice. *J Clin Invest*. 2012;122(3):1052–1065.
16. Barker N. Adult intestinal stem cells: critical drivers of epithelial homeostasis and regeneration. *Nat Rev Mol Cell Biol*. 2014;15(1):19–33.
17. Snippert HJ, van der Flier LG, Sato T, et al. Intestinal crypt homeostasis results from neutral competition between symmetrically dividing Lgr5 stem cells. *Cell*. 2010;143(1):134–144.
18. van Es JH, Sato T, van de Wetering M, et al. Dll1<sup>+</sup> secretory progenitor cells revert to stem cells upon crypt damage. *Nat Cell Biol*. 2012;14(10):1099–1104.
19. Schwitalla S, Fingerle AA, Cammareri P, et al. Intestinal tumorigenesis initiated by dedifferentiation and acquisition of stem-cell-like properties. *Cell*. 2013;152(1–2):25–38.
20. Cui Y, Riedlinger G, Miyoshi K, et al. Inactivation of Stat 5 in mouse mammary epithelium during pregnancy reveals distinct functions in cell proliferation, survival, and differentiation. *Mol Cell Biol*. 2004;24(18):8037–8047.
21. el Marjou F, Janssen KP, Chang BH, et al. Tissue-specific and inducible cre-mediated recombination in the gut epithelium. *Genesis*. 2004;39(3):186–193.
22. Kim TH, Escudero S, Shivdasani RA. Intact function of Lgr5 receptor-expressing intestinal stem cells in the absence of Paneth cells. *Proc Natl Acad Sci U S A*. 2012;109(10):3932–3937.
23. Gordziel C, Bratsch J, Moriggl R, et al. Both STAT1 and STAT3 are favourable prognostic determinants in colorectal carcinoma. *Br J Cancer*. 2013;109(1):138–146.
24. Ahadi M, Sokolova A, Brown I, et al. The 2019 World Health Organization Classification of appendiceal, colorectal and anal canal tumours: an update and critical assessment. *Pathology*. 2021;53(4):454–461.
25. Knösel T, Chen Y, Hotovy S, et al. Loss of desmocollin 1-3 and homeobox genes *PITX1* and *CDX2* are associated with tumor progression and survival in colorectal carcinoma. *Int J Colorectal Dis*. 2012;27(11):1391–1399.
26. Zhao M, Xiong X, Ren K, et al. Deficiency in intestinal epithelial O-GlcNAcylation predisposes to gut inflammation. *EMBO Mol Med*. 2018;10(8):e8736.
27. Vignjevic D, Schoumacher M, Gavert N, et al. Fascin, a novel target of beta-catenin-TCF signaling, is expressed at the invasive front of human colon cancer. *Cancer Res*. 2007;67(14):6844–6853.
28. Anderson S, Poudel KR, Roh-Johnson M, et al. MYC-nick promotes cell migration by inducing fascin expression and Cdc42 activation. *Proc Natl Acad Sci U S A*. 2016;113(37):E5481–E5490.
29. Pribluda A, Elyada E, Wiener Z, et al. A senescence-inflammatory switch from cancer-inhibitory to cancer-promoting mechanism. *Cancer Cell*. 2013;24(2):242–256.
30. Gilbert S, Zhang R, Denson L, et al. Enterocyte STAT5 promotes mucosal wound healing via suppression of myosin light chain kinase-mediated loss of barrier function and inflammation. *EMBO Mol Med*. 2012;4(2):109–124.
31. Gilbert S, Nivarthi H, Mayhew CN, et al. Activated STAT5 confers resistance to intestinal injury by increasing intestinal stem cell proliferation and regeneration. *Stem Cell Rep*. 2015;4(2):209–225.
32. Sangiorgi E, Capecchi MR. Bmi1 is expressed *in vivo* in intestinal stem cells. *Nat Genet*. 2008;40(7):915–920.
33. Yan KS, Chia LA, Li X, et al. The intestinal stem cell markers Bmi1 and Lgr5 identify two functionally distinct populations. *Proc Natl Acad Sci U S A*. 2012;109(2):466–471.
34. Withers HR, Elkind MM. Microcolony survival assay for cells of mouse intestinal mucosa exposed to radiation. *Int J Radiat Biol Relat Stud Phys Chem Med*. 1970;17(3):261–267.
35. Montgomery RK, Carlone DL, Richmond CA, et al. Mouse telomerase reverse transcriptase (mTert) expression marks slowly cycling intestinal stem cells. *Proc Natl Acad Sci U S A*. 2011;108(1):179–184.
36. Sato T, Stange DE, Ferrante M, et al. Long-term expansion of epithelial organoids from human colon, adenoma, adenocarcinoma, and Barrett's epithelium. *Gastroenterology*. 2011;141(5):1762–1772.
37. Buczacck SJA, Zecchini HI, Nicholson AM, et al. Intestinal label-retaining cells are secretory precursors expressing Lgr5. *Nature*. 2013;495(7439):65–69.
38. Adolph TE, Tomczak MF, Niederreiter L, et al. Paneth cells as a site of origin for intestinal inflammation. *Nature*. 2013;503(7475):272–276.
39. Risques RA, Lai LA, Brentnall TA, et al. Ulcerative colitis is a disease of accelerated colon aging: evidence from telomere attrition and DNA damage. *Gastroenterology*. 2008;135(2):410–418.
40. Sakamori R, Yu S, Zhang X, et al. CDC42 inhibition suppresses progression of incipient intestinal tumors. *Cancer Res*. 2014;74(19):5480–5492.
41. Schroeter EH, Kisslinger JA, Kopan R. Notch-1 signalling requires ligand-induced proteolytic release of intracellular domain. *Nature*. 1998;393(6683):382–386.
42. Sato T, Vries RG, Snippert HJ, et al. Single Lgr5 stem cells build crypt-villus structures *in vitro* without a mesenchymal niche. *Nature*. 2009;459(7244):262–265.
43. Terzić J, Grivennikov S, Karin E, et al. Inflammation and colon cancer. *Gastroenterology*. 2010;138(6):2101–2114.
44. Nakaya T, Ogawa S, Manabe I, et al. KLF5 regulates the integrity and oncogenicity of intestinal stem cells. *Cancer Res*. 2014;74(10):2882–2891.
45. Wells CD, Fawcett JP, Traweger A, et al. A Rho1/Amot complex regulates the Cdc42 GTPase and apical-polarity proteins in epithelial cells. *Cell*. 2006;125(3):535–548.
46. Van Aelst L, Symons M. Role of Rho family GTPases in epithelial morphogenesis. *Genes Dev*. 2002;16(9):1032–1054.
47. Georgiou M, Marinari E, Burden J, et al. Cdc42, Par6, and aPKC regulate Arp2/3-mediated endocytosis to control local adherens junction stability. *Curr Biol*. 2008;18(21):1631–1638.
48. Bishop AL, Hall A. Rho GTPases and their effector proteins. *Biochem J*. 2000;348(Pt 2):241–255.
49. Lv C, Zhao X, Gu H, et al. Involvement of activated Cdc42 Kinase 1 in colitis and colorectal neoplasms. *Med Sci Mon Int Med J Exp Clin Res*. 2016;22:4794–4802.
50. Zins K, Gunawardhana S, Lucas T, et al. Targeting Cdc42 with the small molecule drug AZA197 suppresses primary colon cancer growth and prolongs survival in a preclinical mouse xenograft model by downregulation of PAK1 activity. *J Transl Med*. 2013;11:295.
51. van Hengel J, D'Hooge P, Hooghe B, et al. Continuous cell injury promotes hepatic tumorigenesis in Cdc42-deficient mouse liver. *Gastroenterology*. 2008;134(3):781–792.
52. Wu X, Quondamatteo F, Lefever T, et al. Cdc 42 controls progenitor cell differentiation and beta-catenin turnover in skin. *Genes Dev*. 2006;20(5):571–585.
53. Walther A, Johnstone E, Swanton C, et al. Genetic prognostic and predictive markers in colorectal cancer. *Nat Rev Cancer*. 2009;9(7):489–499.
54. Rajagopalan H, Bardelli A, Lengauer C, et al. Tumorigenesis: RAF/RAS oncogenes and mismatch-repair status. *Nature*. 2002;418(6901):934.
55. Cho KR, Vogelstein B. Genetic alterations in the adenoma-carcinoma sequence. *Cancer*. 1992;70(6 Suppl):1727–1731.
56. Russo A, Bazan V, Iacopetta B, et al. The TP53 colorectal cancer international collaborative study on the prognostic and predictive significance of p53 mutation: influence of tumor site, type of mutation, and adjuvant treatment. *J Clin Oncol*. 2005;23(30):7518–7528.



57. Barker N, Ridgway RA, van Es JH, et al. Crypt stem cells as the cells-of-origin of intestinal cancer. *Nature*. 2009;457(7229):608–611.
58. Zhang Z, Zhang F, Davis AK, et al. CDC42 controlled apical-basal polarity regulates intestinal stem cell to transit amplifying cell fate transition via YAP-EGF-mTOR signaling. *Cell Rep*. 2022;38(2):110009.
59. Schuijers J, van der Flier LG, van Es J, et al. Robust cre-mediated recombination in small intestinal stem cells utilizing the *Olfm4* locus. *Stem Cell Rep*. 2014;3(2):234–241.
60. Barker N, van Es JH, Kuipers J, et al. Identification of stem cells in small intestine and colon by marker gene *Lgr5*. *Nature*. 2007;449(7165):1003–1007.
61. Crosnier C, Stamatakis D, Lewis J. Organizing cell renewal in the intestine: stem cells, signals and combinatorial control. *Nat Rev Genet*. 2006;7(5):349–359.
62. Korinek V, Barker N, Morin PJ, et al. Constitutive transcriptional activation by a beta-catenin-Tcf complex in *APC*<sup>-/-</sup> colon carcinoma. *Science*. 1997;275(5307):1784–1787.
63. van Es JH, van Gijn ME, Riccio O, et al. Notch/gamma-secretase inhibition turns proliferative cells in intestinal crypts and adenomas into goblet cells. *Nature*. 2005;435(7044):959–963.
64. Junttila MR, Mao W, Wang X, et al. Targeting LGR5+ cells with an antibody-drug conjugate for the treatment of colon cancer. *Sci Transl Med*. 2015;7(314):314ra186.